Dosimetry and Biodistribution of an Iodine-123-Labeled Somatostatin Analog in Patients with Neuroendocrine Tumors

M.K. O'Connor, L.K. Kvols, M.L. Brown, J.C. Hung, R.J. Hayostek, D.S. Cho, and R.J. Vetter

Departments of Radiology, Oncology and Radiation Safety, Mayo Clinic, Rochester, Minnesota

A modified method for the preparation of a radiolabeled analog of somatostatin (^{123}I-octreotide) is described. The pharmacokinetics and dosimetry of this analog were evaluated in patients with neuroendocrine tumors. Thirty patients had multiple blood and urine samples and sequential anterior and posterior whole-body scintigraphy up to 40 hr postinjection of ^{123}I-octreotide. Region of interest analysis of the whole-body images was used to determine organ and tumor doses. The ^{123}I-octreotide was rapidly cleared from the blood with a $T_{½}$ of 10 min by the hepatobiliary system. By 40 hr, approximately 55% was eliminated in the feces. The gallbladder wall received the highest dose (0.48 rad/mCi), with other organs receiving doses of 0.12 rad/mCi or less. Tumors were identified in 25 of 28 satisfactory studies. Tumor doses ranged from 0.1 to 0.6 rad/mCi. Calculations with ^{131}I instead of ^{123}I indicated that the gallbladder wall would receive 2 rad/mCi, while average tumor doses would range from 0.9 to 5.0 rad/mCi. Iodine-123-octreotide is a useful agent for the visualization of neuroendocrine tumors. The rapid washout of this agent from tumors precludes the possibility of radiotherapy with ^{131}I-octreotide in these patients.

J Nucl Med 1992; 33:1613–1619

Somatostatin is a neuroregulatory peptide, synthesized in a wide variety of human tissues, which acts as a neurotransmitter or hormone with systemic or local effects (*1*). Cell membrane receptors with a high affinity for somatostatin have been shown to be present in the majority of neuroendocrine tumors including carcinoids, islet cell carcinomas and GH producing pituitary adenomas (*2,3*). Large numbers of binding sites have also been reported in other tumors such as meningiomas, breast carcinomas, astrocytomas and oat cell carcinomas of the lung (*4*).

A synthetic analog of somatostatin, octreotide (Sandostatin, Sandoz, Switzerland), shares common structural features, such as the site active in receptor binding, with native somatostatin (*5*). Octreotide has a biologic half-time of 2–3 hr (*6*) compared to 2–3 min for natural somatostatin and has been shown to be effective in controlling symptoms such as flushing and diarrhea in patients with carcinoid syndrome (*7*).

Substitution of a tyrosine molecule in position 3 permits labeling of octreotide with ^{123}I (*8*). Recent studies in both animals and humans have shown that ^{123}I-octreotide successfully imaged tumors with positive receptors for somatostatin (*9–14*) and may be a useful tool in identifying patients who will be responsive to octreotide therapy (*11, 15,16*).

The purpose of this study was to evaluate the pharmacokinetics and dosimetry of ^{123}I-octreotide in patients with known neuroendocrine tumors and to assess the feasibility of an ^{131}I-labeled somatostatin analog for therapeutic applications in the future.

PATIENTS AND METHODS

Patients

A total of 30 patients were studied (12 male, 18 female) with an average age of 52 ± 14 yr. All patients had a histologically or cytologically confirmed diagnosis of neuroendocrine tumor. No significant hepatic or renal dysfunction was present in any patient. Table 1 provides a breakdown of the final diagnosis in each patient. All patients gave informed consent. The study was approved by the institutional review board and the radioactive drug research committee of Mayo Foundation.

Preparation of ^{123}I-Octreotide

Tyr-octreotide was obtained from Sandoz Research Institute (Berne, Switzerland) and its purity confirmed by amino acid sequence and high-pressure liquid chromatography (HPLC). In the first 15 studies, the octreotide was labeled with ^{123}I by the chloramine-T reaction (*17*) using the method of Bakker et al. (*9*). However, this led to large variations in labeling efficiency and modifications were made to previously published methods (*9,18*).

The principal modification was the use of ^{123}I (Nordion Inter., Ontario, Canada) in dry form to increase its specific activity over that available in liquid form. The dry form of ^{123}I had a specific activity of 500 Ci/mg and a radiochemical purity of > 99.8% at 24 hr post-processing. The dry ^{123}I was dissolved in 50 μl 0.5 *M* phosphate-buffer solution and buffered to pH 7 using 1–2 N HCL. The Tyr-octreotide (42 μg in 60 μl of 0.05 *M* acetic acid) was added to the ^{123}I solution and agitated for 30 sec. Radioio-

Received Jan. 14, 1992; revision accepted Apr. 16, 1992.
For reprints contact: Dr. M.K. O'Connor, Section of Nuclear Medicine, Charlton Building, Mayo Clinic, Rochester, MN 55905.

TABLE 1
Final Diagnosis in the 30 Patients Studied

Diagnosis	No. of patients
Carcinoid syndrome	14
Islet cell carcinoma	14
Meningioma	1
Pheochromocytoma	1

dination was initiated by the addition of chloramine-T solution (50 mg in 2 ml of 0.05 *M* phosphate buffer, pH 7.5–7.8) and the solution was vortexed for 1 min. To avoid nonspecific damage to the peptide, the optimum ratio of chloramine-T solution-to-^{123}I solution was found to be 1:23.5. Iodination was terminated by the addition of 1 ml human serum albumin (10%). After vortexing for 30 sec, 10 ml of 0.05 m*M* ammonium acetate was added.

Purification and Quality Control of ^{123}I-Octreotide

The ^{123}I-octreotide iodination solution was purified using a SEP-PAK C18 cartridge (Waters Assoc, Milford, MA). The cartridge was presterilized with 5 ml 70% ethanol and activated with 5 ml 2-propanol. After application of the solution, the cartridge was successively washed with 5 ml fractions of distilled H_2O, 0.5 *M* acetic acid and 96% ethanol. The ethanol fraction was evaporated at 40–50 °C under nitrogen flow and redissolved in 2–5 ml of 0.05 *M* acetic acid in 0.9% NaCl. The ^{123}I-octreotide solution was then passed through a 0.2 μm filter (Acrodisc 13, Gelman Sciences, Ann Arbor, MI) prior to quality control and injection.

The ^{123}I-octreotide preparation was analyzed using a reversed-phase column HPLC system as described previously (*9*). Eluant radioactivity was measured with a NaI probe connected to an analyzer (Model 427, Beckman Instruments, San Ramon, CA).

Patient Preparation and Injection

All patients who were taking octreotide therapeutically were requested to discontinue treatment for a period of 3 wk prior to the start of the study. Five drops per day of Lugol's solution was administered 1 day prior to and for 3 days following the injection of ^{123}I-octreotide. The injected activities were 13.1 ± 5.8 mCi (mean ± s.d.), with a range of 2.1 to 22.2 mCi, in the first 15 patients, and 18.5 ± 2.7 (mean ± s.d.) with a range of 14.7 to 24.0 mCi in the remaining 15 patients. Poor labeling efficiency and low injected activities lead to suboptimal image quality in two of the first 15 cases and analysis of these data has been excluded from the results. Depending upon the labeling efficiency, patients received less than 35 μg of radiolabeled octreotide. The radiopharmaceutical was injected via a peripheral arm vein over a 5-min period. Starting 4–6 hr after injection of the ^{123}I-octreotide, four liters of Golytely were administered orally over a 2-4-hr period to aid in the clearance of radioactivity excreted into the bowel via the hepatobiliary system.

Patient Imaging

Planar images were acquired using a dual-headed gamma camera system (Bodyscan, Siemens Gammasonics, Des Plaines, IL). The gamma camera heads were equipped with low-energy, high-resolution collimators and images were acquired using a 20% window centered on the 159 keV emission from ^{123}I. Following injection, images of the abdomen were acquired at 1 min/image for 60 min. Data were stored on the computer in a 64 × 64 word mode matrix (Pinnacle System, Medasys, Ann Arbor, MI). Anterior and posterior whole-body images were then acquired at 1, 2 and 4 hr postinjection (20 min acquisition) and again at 16 and 40 hr (40 min acquisition). All whole-body images were stored on the computer in 1024 × 256 word mode matrix.

Iodine-123-octreotide is excreted by the hepatobiliary system. If required, patients were given Sincalide (CCK octapeptide, 0.02 μg/kg) to reduce gallbladder activity following the initial whole-body scan. SPECT imaging of the liver was performed between the 2- and 4-hr whole-body acquisitions. Data were acquired on a LFOV gamma camera (Starcam, GE, Milwaukee, WI) equipped with a low-energy, high-resolution collimator. Sixty-four images were acquired in a 128 × 128 matrix at 40 sec/image. The planar images were prefiltered with a Hann filter (cut-off = 0.4 × Nyquist) and backprojected with a ramp filter. Occasionally, SPECT of other sites was obtained to further evaluate regions of known disease or unexpected activity. In some patients, high gallbladder activity led to corruption of surrounding structures in the liver, despite the administration of Sincalide. To eliminate this problem, the gallbladder was subtracted from the planar data prior to reconstruction using the method of Gillen et al. (*19*).

Blood and Urine Collection

Blood and urine samples were collected in 10 of the 30 patients. Blood samples were collected at 1, 5, 10, 20 and 30 min and at 1, 2, 4, 16 and 40 hr postinjection. Complete urine samples were also collected in 12-hr increments up to 40 hr postinjection. The radioactivity in blood and urine was measured using a gamma counter (Minaxi 5000, Packard, IL) and expressed as a percentage of administered activity.

Data Analysis and Dosimetry

From the 1-hr dynamic study, a region of interest (ROI) was drawn over the liver and a time-activity curve was generated to determine the rate of uptake of ^{123}I-octreotide.

Geometric mean images were created from each set of anterior and posterior whole-body images. An ROI was drawn outside the body to determine background counts and true whole-body counts were then calculated. Whole-body counts were then corrected for decay of the ^{123}I and expressed as a percentage of counts in the 1-hr, whole-body image. When the appropriate organs were visualized, ROIs were drawn over all tumor regions, liver, gallbladder, small bowel, upper large intestine, lower large intestine, lungs, thyroid, kidneys and bladder. Background correction was performed using a region of soft tissue in the upper thigh. ROI counts were decay-corrected and expressed as a percentage of the whole-body counts in the 1-hr image. The biological half-times and intercepts for the above organs and the whole body were calculated using the PLOT subroutine of MIRDOSE (*20*). The effective half-time and intercept were used in the following equation to obtain the residence time, τ, for each organ:

$$\tau = 1.443\ T_e\ f,$$

where T_e is the effective half-time for each compartment and f is the intercept of the compartment. Organ dose (D) was calculated by the absorbed fraction method (*21*), using the MIRDOSE program, by summing the contributions from each organ:

$$D = \sum \tau\ S,$$

where S is the target organ dose-rate per unit of activity in each organ. The effective dose equivalent was calculated by the method of ICRP 26 (*22*).

In MIRDOSE, the dynamic bladder model was utilized with a voiding interval of 4.8 hr and the results compared to those obtained with the ROI data. MIRDOSE also allows the selection of a gastrointestinal (GI) kinetics model described in ICRP 30 (*23*). Normal GI kinetics were assumed and the ICRP kinetics model was utilized and compared to dose estimates computed from ROI data.

For all tumors, the height and width of the lesions were measured from the appropriate anterior or posterior image and tumor volume calculated by assuming a spherical, ellipsoidal or cylindrical shape for the lesion. It is recognized that this method is not ideal and provides, at best, a crude estimate of tumor volume.

With the assumption that the biological behavior of radioiodinated tyr-octreotide is independent of the isotope used, organ and tumor doses for ^{131}I-octreotide were calculated from the biological data obtained from ^{123}I-octreotide. For ^{131}I, it was assumed that all beta energy (mean = 0.19 Mev) would be absorbed in the tumor. The beta dose, R_β, was calculated from the following equation:

$$R_\beta = 73.8\ (0.19\ \text{Mev})\ T_e,$$

where T_e is the effective half-time, in days, of ^{131}I in the tumors. For gamma rays, absorbed fractions were estimated from Table 8, MIRD Pamphlet 2 (*24*), for tumor sizes that approximate those in study patients and used to compute the gamma ray dose R_γ to the tumor. This dose was added to the beta absorbed dose for each tumor to give total tumor dose in g-rads/μCi.

RESULTS

Labeling Efficiency

In the first 15 patients, 33.7% ± 12.4% was recovered as ^{123}I-octreotide in the 96% ethanol solution. Hence, initial activities of 60 mCi ^{123}I were required per study. With the modifications to the labeling procedure described above, the recovered activity increased to 65.6% ± 5.4% in the remaining 15 patients, requiring an initial activity of only 30 mCi per study. HPLC analysis showed 99.2% ± 0.8% of the injected activity to be ^{123}I-octreotide.

Pharmacokinetics

Results from the 10 patients in whom complete blood and urine samples were obtained are presented in Figures 1–2. Figure 1 shows the percent injected ^{123}I in whole blood and the initial hepatic uptake of ^{123}I over the first 60 min postinjection. Activity left the vascular compartment with a calculated $T_{½}$ of 10 min with only 10% remaining after 1 hr. Thereafter blood activity decreased more slowly with approximately 4% present at 24 hours postinjection. Peak hepatic uptake occurred approximately 20 min postinjection and thereafter washed out with a $T_{½}$ of 105 ± 35 min (mean ± s.d.).

Figure 2 shows the whole body distribution of ^{123}I-octreotide over a 40-hr period. The combined whole body and urine activity at 1 hr postinjection was considered to represent 100% of the injected activity. The difference between the combined whole body and urine activity at other times postinjection was attributed to loss of activity in the feces. Fecal excretion was the principal mode of elimination from the body, with approximately 55% lost in the feces by 40 hr postinjection.

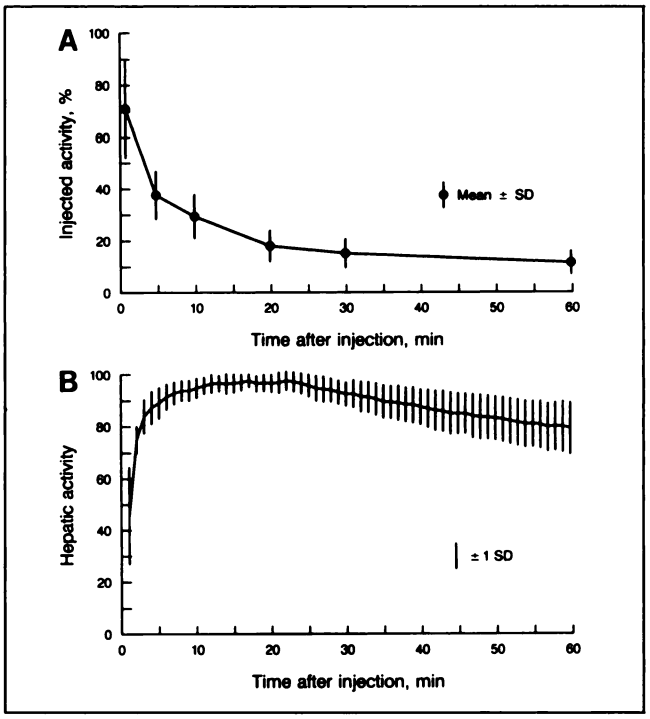

FIGURE 1. (A) Percent of the injected activity of ^{123}I-octreotide in whole blood over the first hour postinjection. (B) Relative uptake of ^{123}I-octreotide in the liver following injection (normalized to maximum hepatic activity for each subject).

Figure 3 presents examples of anterior and posterior whole-body images of ^{123}I-octreotide distribution at 2 and 40 hr postinjection in a patient with islet cell carcinoma of the pancreas. The patient had multiple liver lesions demonstrated on CT and MRI scans. Scintigraphy failed to show these lesions, but the images are useful in dem-

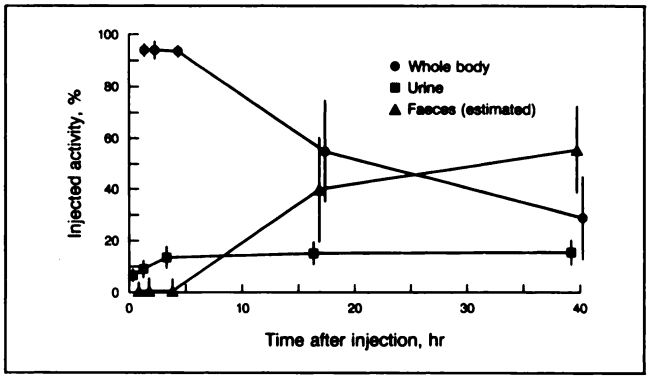

FIGURE 2. Distribution of ^{123}I-octreotide in the whole body, urine and feces over the first 40 hr postinjection.

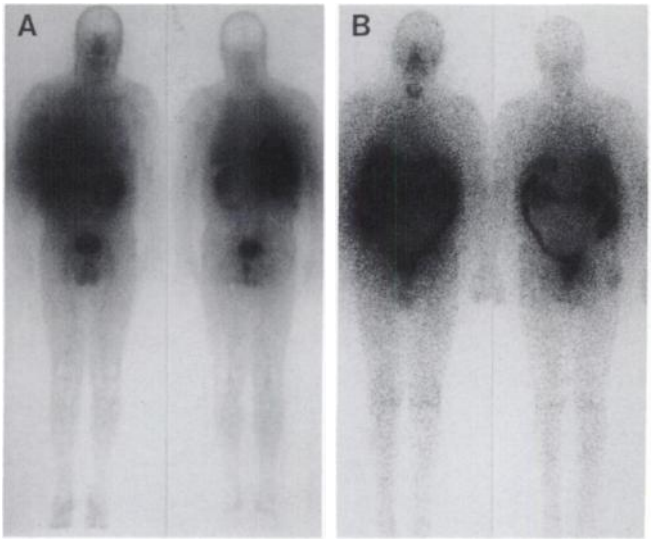

FIGURE 3. Anterior and posterior whole-body images taken at (A) 2 hr and (B) 40 hr postinjection illustrate the biodistribution of ^{123}I-octreotide.

onstrating the changing whole-body distribution of ^{123}I-octreotide over time. On the 2-hr images (Fig. 3A), there was intense gallbladder activity along with activity in the liver, bladder, kidneys and lungs. There was no significant activity in the bone marrow or any other soft-tissue region. The 40-hr images (Fig. 3B) show activity primarily located in the large bowel, with activity still present in the liver and kidneys. Activity can also be seen in the thyroid. Thyroid uptake was seen on several patients despite adequate blockage with Lugol's solution. This may be due to the presence of somatostatin receptors in the thyroid gland.

The biodistribution of ^{123}I-octreotide in the 28 patient studies is shown in Figure 4. Approximately 20%–30% appears in the liver and gastrointestinal system (Fig. 4A), with less than 4% in the kidney and bladder. Lung uptake was noted in the early (1–4 hr) images (Fig. 3), however the values of 3%–4% presented in Figure 4B may be an overestimation since no attenuation correction was applied to the data.

Figure 5A shows the ^{123}I-octreotide images taken 4 hr postinjection in a patient who developed omental metastases 2 yr after resection of a small bowel carcinoid. The patient developed progressive carcinoid syndrome with extensive hepatic metastases seen on CT scan, which were also seen on SPECT somatostatin images (not shown). These lesions are just discernable as areas of irregular activity in Figure 5A. Uptake was also seen in the mediastinum, left supraclavicular region and right femur. A subsequent bone scan (Fig. 5B) confirmed the lesion in the right femur to be an osseous metastasis.

In the 28 patients, 22 had positive scans with uptake in hepatic tumors (17 patients) and nonhepatic tumors (10 patients). Three patients showed photon-deficient uptake in known tumor regions and three patients had negative scans. Estimated tumor volumes were 14.6 ± 18.2 g (range

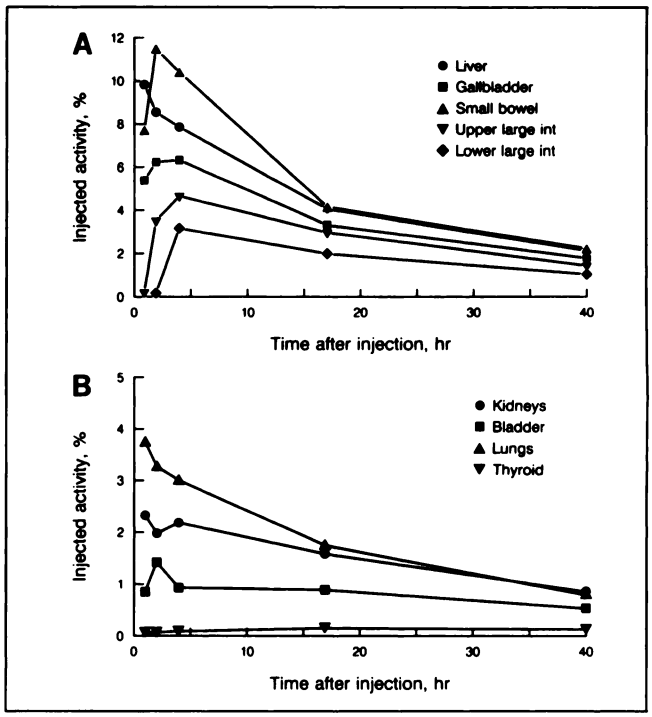

FIGURE 4. Mean values in 28 patients of the percent of the injected activity of ^{123}I-octreotide in (A) the liver and gastrointestinal system and (B) the lungs, thyroid and genitourinary system over the first 40 hr postinjection.

1–59 g) for nonhepatic lesions and 385 ± 433 g (range 9–1130 g) for hepatic lesions. For analysis of washout of activity from tumors, the percent uptake of ^{123}I-octreotide in 25 nonhepatic lesions and 6 hepatic lesions was measured over the 40-hr scanning period. Figure 6 indicates that washout of activity from tumors was similar for both

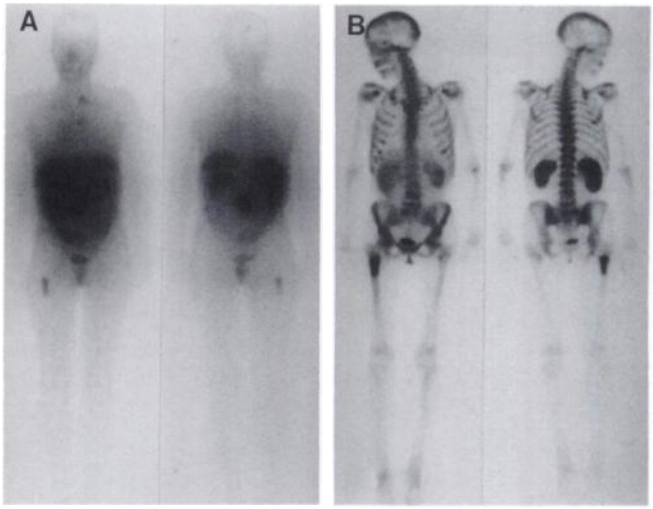

FIGURE 5. (A) Anterior and posterior whole-body images at 4 hr postinjection. Uptake is seen in the mediastinum, the left supraclavicular region and the proximal right femur. (B) Bone scan demonstrates a focal area of increased uptake in the proximal right femur corresponding to the metastatic lesion seen on the ^{123}I-octreotide scan.

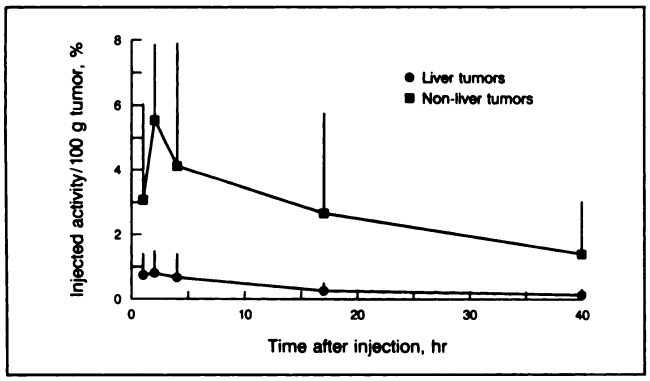

FIGURE 6. Uptake and washout of ^{123}I-octreotide in hepatic and nonhepatic tumors. Results have been normalized to %injected activity per 100 g tumor tissue (for clarity, only mean + s.d. is shown).

hepatic and nonhepatic lesions, with a biological half-time of approximately 15 hr for hepatic tumors and 22 hr for nonhepatic tumors. However, tumor uptake per gram of tissue was greater (by a factor of approximately 6–7) in nonhepatic lesions as compared to hepatic lesions.

Dosimetry

Table 2 presents the absorbed dose estimates in various organs and the effective dose for ^{123}I-octreotide. The highest dose is to the gallbladder wall with an absorbed dose of approximately 0.5 rad/mCi. Results obtained using the MIRDOSE bladder model gave a dose of 0.066 rad/mCi to the bladder wall. This value compares well with the value of 0.068 rad/mCi obtained from the ROI data. The ICRP model of GI kinetics gave dose estimates to the upper and lower large intestine, which were approximately an order of magnitude larger than those computed from the ROI data (Table 2). The mean effective dose for the 28 studies was in the range 0.07–0.22 rem/mCi, which compares favorably with other radiopharmaceuticals.

Tumor dose (data not shown) varied with tumor location (hepatic versus nonhepatic) and was reduced by a factor of 3 in large hepatic lesions (>150 ml) relative to nonhepatic lesions. The tumor doses ranged between 0.1–0.6 rad/mCi, which are not significantly larger than the dose to the gallbladder.

Table 3 presents the dose estimates to the body from ^{131}I-octreotide, calculated using the biological data from ^{123}I-octreotide. From the ROI data, the highest dose is to the gallbladder wall, which receives a dose of 2.2 rad/mCi. Under conditions where normal GI kinetics are applicable, the highest dose is to the lower large intestine, which receives a dose of 16.4 rad/mCi.

Table 4 shows the calculated absorbed dose to tumors for ^{131}I-octreotide, expressed as g-rads per μCi of activity in the tumor. Using average tumor volumes of 20 g and 350 g, and uptakes of 5.5% and 0.8% per 100 g tumor

TABLE 2
Estimated Mean Organ Dose and Effective Dose from ^{123}I-Octreotide Computed Using ROI Data (ROI) and ICRP Gastrointestinal Kinetic Model + MIRDOSE Dynamic Bladder Model (GI/DBM)

Target organ	ROI rad/mCi	GI/DBM rad/mCi
Gallbladder wall	0.48	0.53
Liver	0.10	0.11
Small intestine	0.11	0.32
Upper large intestine	0.10	0.77
Lower large intestine	0.08	0.86
Kidneys	0.12	0.14
Urinary bladder wall	0.07	0.10
Thyroid	0.11	0.11
Lungs	0.06	0.06
Breast	0.02	0.03
Ovaries	0.06	0.19
Testes	0.03	0.04
Red marrow	0.04	0.05
Bone surfaces	0.06	0.07
Effective dose H(E) female	0.08	0.22
Effective dose H(E) male	0.07	0.18

TABLE 3
Estimated Mean Organ Dose from ^{131}I-Octreotide Based on the Kinetic Behavior of ^{123}I-Octreotide and Computed Using ROI Data (ROI) and ICRP Gastrointestinal Kinetic Model + MIRDOSE Dynamic Bladder Model (GI/DBM)

Target organ	ROI rad/mCi	GI/DBM rad/mCi
Gallbladder wall	2.17	2.37
Liver	0.33	0.39
Small intestine	0.44	1.67
Upper large intestine	0.32	6.40
Lower large intestine	0.32	16.40
Kidneys	0.49	0.58
Urinary bladder wall	0.46	0.69
Thyroid	0.50	0.50
Lungs	0.22	0.22
Breast	0.09	0.09
Ovaries	0.15	0.83
Testes	0.10	0.16
Red marrow	0.25	0.13
Bone surfaces	0.17	0.11

TABLE 4
Estimated Tumor Dose for ^{131}I-Octreotide Expressed as g-rad per μCi of Activity in the Tumor

Tumor size (g)	Hepatic tumors		Nonhepatic tumors	
	R_γ	$R_{\gamma+\beta}$	R_γ	$R_{\gamma+\beta}$
2	0.2	8.8	0.2	12.9
20	0.9	9.5	0.9	13.6
50	1.1	9.7	1.1	13.8
150	1.5	10.1		
350	2.1	10.7		
700	2.6	11.2		
1100	3.0	11.6		

Largest nonhepatic tumor was 59 g.

tissue for nonhepatic and hepatic tumors respectively, the average tumor doses were calculated to be 5 rad/mCi and 0.9 rad/mCi for nonhepatic and hepatic lesions, respectively. These tumor doses are of the same order of magnitude as doses to target organs.

DISCUSSION

A review of our labeling procedure indicated that the radioiodination of tyr-octreotide was best performed in a small volume (30–200 μl) to permit efficient radioiodination of minute amounts of protein/peptide. Bakker et al. (*9*) observed some instances of low labeling yields (<5%) with ^{123}I-octreotide which they attributed to other iodine impurities and the low specific activity of ^{123}I (<100 Ci/mg). We experienced similar problems, which were resolved by the use of very high specific activity ^{123}I. The high peptide-to-iodine ratio (4200:1) not only favors a higher radioiodination, but also avoids the formation of di-iodinated tyr-octreotide (*9*). Furthermore, the concentration and duration of exposure of the tyr-octreotide to chloramine-T was kept to a minimum to avoid nonspecific damage to the protein/peptide.

The HPLC analysis indicated that the radioiodinated peptide separated by SEP-PAK C18 cartridge contained very high purity ^{123}I-octreotide. This suggests that SEP-PAK C18 chromatography can be utilized for the purification and quality control of ^{123}I-octreotide without the additional need of using a HPLC system.

While the initial in-vivo behavior of ^{123}I-octreotide as shown in Figure 1 is similar to that reported by Bakker et al. (*12*), we found significant differences in the pathway by which the radiolabeled somatostatin was eliminated from the body. The study of Bakker et al. (*12*) found a high urinary excretion (approximately 45% in the first 30 hr) with little or no fecal excretion of the ^{123}I-octreotide in patients with normal gastrointestinal function (i.e., no previous intestinal operations). They concluded that the radiolabeled octreotide was hydrolyzed in the intestines and the degradation products reabsorbed. In contrast, our results indicated that fecal excretion accounted for 55% of the administered dose over the first 40 hr, with only 15%–20% accounted for by urinary excretion (Fig. 4). Activity in the large bowel was commonly observed in the 16- and 40-hr images (Fig. 3), and could sometimes be seen in the 4-hr images (Fig. 6). The main reason for these discrepancies may be due to the use in this study of a cathartic (Golytely) that induced water diarrhea and would have shortened the residence time of radioactivity in the small and large bowel. This shortened residence time would also have reduced the degree to which the ^{123}I-octreotide could be hydrolyzed and reabsorbed in the intestines.

The use of simultaneous anterior and posterior whole-body imaging permitted a more accurate estimate of the biodistribution of ^{123}I-octreotide than previously reported (*12*). While most activity was localized in the GI system, uptake was also seen in the genitourinary system and in the lungs (Fig. 3). At present, we do not have a satisfactory explanation for this pulmonary uptake. Dose estimates to various organs in the body, based on ROI data, indicate that the highest dose is to the gallbladder wall which receives a dose of 480 mrad/mCi (Table 2). This is in good agreement with the value of 440 mrad/mCi obtained by Bakker et al. (*12*). The GI kinetic model from ICRP 30 indicates that the highest dose should be to the upper and lower large intestine, which would receive approximately 800 mrad/mCi (Table 2). This more conservative dose estimate assumes that normal gastrointestinal kinetics are applicable. However, due to the administration of a cathartic, our results would indicate that gastrointestinal transit is more rapid than normal and consequently the ICRP 30 kinetic model is not applicable in this study. Hence, the use of a cathartic has two primary benefits in ^{123}I-octreotide scintigraphy: reduced background activity in the abdominal region and a major reduction in the radiation dose to the small and large intestines.

The uptake and washout of ^{123}I-octreotide in tumors was very similar to that seen in the liver and gastrointestinal tract, with the maximum uptake occurring between 1–4 hr postinjection. We found a significant difference in the absolute uptake of ^{123}I-octreotide by hepatic and nonhepatic tumors (Fig. 6). This may be due to differences in tumor cell density in hepatic versus nonhepatic lesions. The results presented in Tables 3 and 4 indicate that the average tumor dose with ^{131}I-octreotide is of the same order of magnitude as doses to the gallbladder, kidneys and thyroid, due to the similarity in kinetics of ^{123}I-octreotide in normal body organs and in tumors. Hence, the therapeutic application of tyr-octreotide labeled with ^{131}I- or ^{125}I does not appear feasible. It is possible that other formulations of radiolabeled somatostatin, with longer tumor retention times, may have potential therapeutic applications.

The feasibility of labeling somatostatin or an analog of somatostatin with other radioisotopes has been investigated by several groups, and initial studies with both ^{111}In (*25,26*) and ^{99m}Tc-labeled analog of somatostatin (*27*) have shown promising results. In particular, results with ^{111}In-DTPA-octreotide have indicated that this agent may be superior to ^{123}I-octreotide, due to reduced background activity in the abdomen and consequential improvement in the visualization of abdominal lesions (*26*).

In conclusion, we have found that ^{123}I-octreotide is a useful agent for the visualization of neuroendocrine tumors. It demonstrates a favorable dosimetry, comparable to many existing diagnostic radiopharmaceuticals. Its rapid uptake permits imaging within 1–4 hr postinjection. However, the rapid washout of this agent from the tumor site precludes the possible therapeutic applications of tyr-octreotide radiolabeled with isotopes such as ^{131}I or ^{125}I.

REFERENCES

1. Reichlin S. Somatostatin. *N Engl J Med* 1983;309:1495–1501, 1556–1563.

2. Reubi JC, Kvols LK, Krenning E, Lamberts SWJ. Distribution of somatostatin receptors in normal and tumour tissue. *Metabolism* 1990; 30(suppl 2):78–81.
3. Reubi JC, Hacki WH, Lamberts SWL. Hormone-producing gastrointestinal tumours contain high density of somatostatin receptors. *J Clin Endocrinol Metab* 1987;65:1127–1134.
4. Reubi JC, Kvols LK, Nagorney DM, et al. Detection of somatostatin receptors in surgical and percutaneous needle biopsy samples of carcinoids and islet cell carcinomas. *Cancer Res* 1990;50:5969–5977.
5. Bauer W, Briner U, Doepfner WS, et al. SMS 201-995: a very potent and selective octapeptide analogue of somatostatin with prolonged action. *Life Sci* 1982;31:1133–1141.
6. Kvols LK, O'Dorisio T, Patel S, Peterson D, Gilbertson D, Moertel C. Pharmacokinetic studies of SMS 201-995 (Sandostatin) comparing two subcutaneous injection sites. *J Natl Cancer Inst* 1989;81:1926–1929.
7. Kvols LK, Moertel CG, O'Connell MJ, Schutt AJ, Rubin J, Hahn RG. Treatment of the malignant carcinoid syndrome: evaluation of a long acting somatostatin analogue. *N Engl J Med* 1986;315:663–666.
8. Reubi JC. New specific radioligand for one subpopulation of brain somatostatin receptors. *Life Sci* 1985;36:1829–1836.
9. Bakker WH, Krenning EP, Breeman WA, et al. Receptor scintigraphy with a radioiodinated somatostatin analogue: radiolabeling, purification, biologic activity, and in vivo application in animals. *J Nucl Med* 1990;31: 1501–1509.
10. Krenning EP, Bakker WH, Breeman WAP, et al. Localization of endocrine-related tumours with radioiodinated analogue of somatostatin. *Lancet* 1989;1:242–244.
11. Lamberts SWJ, Bakker WH, Reubi JC, Krenning EP. Somatostatin-receptor imaging in the localization of endocrine tumors. *N Engl J Med* 1990; 323:1246–1249.
12. Bakker WH, Krenning EP, Breeman WA, et al. In vivo use of a radioiodinated somatostatin analogue: dynamics, metabolism, and binding to somatostatin receptor-positive tumors in man. *J Nucl Med* 1991;32: 1184–1189.
13. Kwekkeboom DJ, Krenning EP, Bakker WH, et al. Radioiodinated somatostatin analog scintigraphy in small-cell lung cancer. *J Nucl Med* 1991; 32:1845–1848.
14. Bihl H, Sterz M, Macke H, Eisenhut M, Rath U. Somatostatin receptor scintigraphy: a new scintigraphic tool in the management of intestinal carcinoids [Abstract]. *Eur J Nucl Med* 1991;18:577.
15. Ur E, Bomanji J, Mather SJ, Britton KE, Grossman A, Besser GM. Somatostatin-receptor imaging in acromegaly [Abstract]. *Eur J Nucl Med* 1991;18:558.
16. Becker W, Mariehagen J, Scheubel R, et al. I-123-labelled tyr-3-octreotide scans in endocrine neoplasms [Abstract]. *Eur J Nucl Med* 1991;18:559.
17. Hunter WM, Greenwood FC. Preparation of iodine-131 labeled human growth hormones of high specific activity. *Nature* 1962;194:495–496.
18. Djura P, Hoskinson RM. ^{123}I-somatostatin analogues: high-performance liquid chromatography profiles and antibody binding properties following three methods of radioiodination. *J Chromatogr* 1987;389:261–266.
19. Gillen GJ, McKillop JH, Hilditch TE, Davidson JK, Elliott AT. Digital filtering of the bladder in SPECT bone studies of the pelvis. *J Nucl Med* 1988;29:1587–1595.
20. Watson EE, Stabin MG, Bolch WE. *MIRDOSE.* Oak Ridge, TN: Oak Ridge Associated Universities; 1984.
21. Loevinger R, Budinger TF, Watson EE. *MIRD Primer for absorbed dose calculations.* New York: The Society of Nuclear Medicine; 1988.
22. International Commission on Radiological Protection. Recommendations of the International Commission on Radiological Protection. *ICRP publication 26.* New York: Pergamon Press; 1977.
23. International Commission on Radiological Protection. Limits for intakes of radionuclides by radiation workers. *ICRP publication 30, part I.* New York: Pergamon Press; 1978.
24. Berger MJ. Energy deposition in water by photons from point isotropic sources. MIRD Pamphlet 2. *J Nucl Med* 1968;9(suppl 1).
25. Kooij PPM, Bakker WH, Breeman WAP, et al. Human radiation dosimetry of [In-111-DTPA-D-Phe]-octreotide, a new imaging agent for the detection of somatostatin receptor-positive tumors [Abstract]. *J Nucl Med* 1991;32: 1043.
26. Kwekkeboom DJ, Oei HY, Bakker WH, et al. [In-111-DTPA-D-Phe]-octreotide scintigraphy in neuro-endocrine tumors [Abstract]. *J Nucl Med* 1991;32:981.
27. Cox PH, Pillay M, Schonfeld DHW. Technetium-labelled somatostatin for in vivo tumour localization [Abstract]. *Eur J Nucl Med* 1991;18:558.

CORRECTION

In the July issue of the *Journal*, the title of the article by Mehta et al. (pages 1373–1377) was printed incorrectly. The corrected title is: In-Vivo Identification of Tumor Multidrug Resistance with ^{3}H-Colchicine.